Supplementary information for

Greenhouse gas emissions from boreal inland waters unchanged after forest harvesting

Marcus Klaus[1*], Erik Geibrink[1], Anders Jonsson[1], Ann-Kristin Bergström[1], David Bastviken[2], Hjalmar Laudon[3], Jonatan Klaminder[1], Jan Karlsson[1]

[1]Department of Ecology and Environmental Science, Umeå University, SE-90187 Umeå, Sweden
[2] The Department of Thematic Studies - Environmental Change, Linköping University, SE-58183 Linköping, Sweden
[3]Department of Forest Ecology and Management, Swedish University of Agricultural Science, SE-90183 Umeå, Sweden

Correspondence to: Marcus Klaus (marcus.klaus@posteo.net)

Text S1 Sampling and analysis of dissolved gases

Partial pressure of CO_2 in stream and lake surface waters was measured by a hand held non-dispersive infra-red CO_2 sensor (GM70 Carbon dioxide meter, Vaisala Inc. Helsinki, Finland) or an infrared gas analyzer (IRGA EMG-4, PP-Systems Inc., Amesbury, MA, U.S.) coupled to a gas equilibrator (MINIMODULE 1.7 x 5.5 G542, Membrana Liqui-Cel Inc., Wuppertal, Germany) through which sample water was transferred by a peristaltic pump (Master-Flex 7518-12, Cole-Parmer Instrument Company, East Bunker Ct Vernon-Hills, IL, USA). Both CO_2 sensors were calibrated monthly against reference gas mixtures (AGA, Linde AG). Molar CO_2 concentrations were derived from Henry's law constants using water temperature-parameterizations in Wanninkhof (1992). For DIC and CH_4 sampling, 4 ml of water was injected into gas-tight 22 ml glass vials (Perkin Elmer Inc., Waltham, MA, USA) containing 50 µl 1.2M HCl, sealed with 20 mm natural pink rubber stoppers flushed with N_2 gas prior to sampling. For N_2O sampling we used the headspace equilibration technique where 50 ml of headspace gas (air taken in upwind direction 2 m aboveground) was equilibrated with 540 ml of surface water by vigorous shaking for 1 min and then transferred to a glass vial (as described above, but here without HCl) allowing any overpressure to be released during gas injection. CO_2, CH_4 and N_2O concentrations in the vial headspace were analyzed using a gas chromatograph (GC, Clarus 500, Perkin Elmer Inc., Waltham, MA, USA) equipped with a methanizer and flame ionization detector (for CH_4 analysis) and an electron capture detector (for N_2O analysis). Headspace concentrations were converted to molar concentrations by means of the ideal gas law using Bunsen solubility coefficients given in Wanninkhof (1992).

Groundwater was sampled biweekly for nutrient, DIC and CH_4 concentrations from PVC groundwater wells located at two forested hillslope sites (inclination 1-5%), 10-70 m from the impact lakes. The two wells had an inner diameter of 18 mm and were 100 and 110 cm deep with openings across a depth range of 37.5-42.5 cm and 5-105 cm to separate responses in surficial groundwater (depth specific sampling) from general responses in the whole profile (depth integrated sampling). A proportion of 65%-85% of the drainage areas of one of the hillslope sites were affected by forest clear-cutting while the forest in the drainage area of the other sites were left intact (Fig. 2). At each site, groundwater levels were measured and groundwater collected from two wells using a peristaltic pump (Master-Flex 7518-12, Cole-Parmer Instrument Company, East Bunker Ct Vernon-Hills, IL, USA) by carefully transferring it to acid washed plastic bottles. Subsamples for chemical analysis were taken from these bottles immediately after sampling. Parallel sampling of groundwater for DIC and CO_2 concentrations (n=11 per groundwater sampling site) showed that 92±11% (mean±standard deviation) of the DIC pool was CO_2 due to the low pH of <5 (data not shown). Hence, we use DIC as a proxy for groundwater CO_2 concentrations.

Text S2 Logger systems

Surface water CO_2 observations were measured 2-hourly at 10 cm water depth at the deepest point of the lakes and the master stream sites using non-dispersive infra-red CO_2 sensors (CARBOCAP GMP 222, Vaisala Inc., Helsinki, Finland) enclosed in a semi permeable PTFE membrane, coupled to Vaisala GMT 220 transmitters (Johnson et al., 2010) and connected to a data logger (CR200X, Campbell Scientific Inc., Logan, UT, USA). Times series were corrected for sensitivities to temperature and pressure following Johnson et al. (2010) and for linear drifts based on probe-calibrations before and after the field season.

Lake water temperature was measured at 5 min intervals at every 0.5 m (0-3 m depth) or 1-2 m (below 3 m) at the deepest point of the lake using temperature loggers (Hobo TidbiT V2, Onset Inc., Bourne, MA, USA). Stream water height and temperature was measured hourly with a water height data logger (WT-HR 100, Trutrack Inc.), placed at well-defined reaches at the master stream sites (Fig. 2). Water height logger readings were drift-corrected based on biweekly manual water height measurements. Discharge was measured occasionally throughout the whole study period using slug injections based on salt in solution following Moore (2005). Measured discharge was related to water height using rating curves, i.e. piecewise power type equations with one or two segments and segment-specific normalized root mean square errors of 0.10-0.23 at Övre Björntjärn (n=30), 0.31 at Lillsjölidtjärnen (n=33) and 0.19-0.33 at Struptjärn (n=42). The rating curves were used to calculate hourly discharge from logged water height.

Wind speed, relative humidity, air temperature, precipitation and air pressure were measured every 5-10 min at 2.5 m above open mires 100-300 m from Övre Björntjärn, Lillsjölidtjärnen and Struptjärn, respectively (Fig. 2). The mires had about the same size as the lakes and were surrounded by similar vegetation with similar clear-cut buffer zones left aside. Hence, weather measurements on the mires can be regarded to be representative for lake conditions, at least in terms of the relative differences between lakes and years. At Övre Björntjärn and Lillsjölidtjärnen we used mobile weather stations (Hobo U30-NRC, Onset Inc., Bourne, MA, USA). At Struptjärn, wind speed and precipitation was measured using a propeller wane (RM Young wind monitor, R.M. Young Company, MI, USA) and a tipping bucket rain gauge (ARG100, EML Inc., North Shields, UK), respectively, connected to a data logger (CR10, Campbell Scientific Inc., Logan, UT, USA). Air pressure and air temperature was measured every 10 min using a water level logger (Hobo U20 001-01-Ti, Onset Inc., Bourne, MA, USA). Relative humidity was assumed to be the same as at Övre Björntjärn. Weather data with 10 min intervals for Stortjärn was derived from the reference climate monitoring program at Svartberget experimental forest, Vindeln, Sweden, 2 km from Stortjärn (Laudon et al., 2013). Here, wind speed was measured at 16 m above dense spruce forest using a propeller wane. Relative humidity and air temperature was measured at 1.7 m above ground in an open area. Air pressure was scaled from observations at Struptjärn using the barometric formula (Iribarne and Godson, 1981). Light intensity was measured every 10 min using lux meters (Hobo UA-002-64, Onset Inc., Bourne, MA, USA) placed 1 m above ground within 30 m from each lake in an open environment and within 1 m from four of the five stream sampling sites.

Text S3 Gap filling of logger data

Continuously logged data showed occasional gaps (Table S2). For lake CO_2 concentrations, we occasionally observed diel cycles which were greatly exaggerated by biofouling. We identified and gap-filled erroneous patterns based on independently measured covariates (water temperature, lux, wind speed) following a multivariate outlier detection and multiple imputation approach using 10 bootstrap runs, described in detail by Klaus et al. (2017). Stream CO_2 concentrations peaked above the detection limit of the probes (10000 ppm) during extreme summer low-flow in Struptjärn. To avoid extrapolation, we filled these gaps by linear interpolation of spot measurements, assuming an error of ±50%. Gap-filled data totaled 7% of CO_2 measurements in lakes and 3% in streams (Table S2). Missing wind speed data (12%) were gap-filled using a multiple imputation model with variable squared time effects (Honaker et al. 2011) trained for each year with wind speed observations from all other weather stations and carried out using 10 bootstrap runs. Gaps in air temperature, air pressure, relative humidity

and lux data (4-11% of the total record) were filled using linear regression models trained with data from the nearest logger from the respective year (R^2=0.63-0.99, Table S2). Here, time series were subsampled to 8 hour intervals to avoid problems of serial autocorrelation (Breusch-Godfrey test, p>0.05). Gaps in time series of lake thermal characteristics (4% of the total record) were filled using linear regression models trained with data collected in the other replicate lake in the respective year (R^2=0.60-0.96). Here, time series were subsampled to 10 day intervals to avoid problems of serial autocorrelation (Breusch-Godfrey test, p>0.05).

Text S4 Gas transfer velocity measurements in streams

Air-water gas transfer rates in streams were measured using a static polymethylmethacrylate gas flux chamber (60 x 20 x 23 cm^3) with a hexagonal base and rounded edges to minimize chamber induced turbulence (Fig. S1). For each gas flux measurement, the chamber was mounted to a tripod and placed onto the water surface centered in the stream with the main axis oriented in flow direction and the side walls extending 2 cm into the water. CO_2 concentrations in the chamber were measured using a CO_2 logger (CO2 Engine® ELG, SenseAir AB, Delsbo, Sweden, Accuracy = ± 30 ppm ± 3 % of measured value, response time <25 s) that was off-set calibrated against N_2 gas before each field visit. The CO_2 logger was mounted on top of the chamber and connected to a pump (SP 270 EC-LC 12VDC, Schwarzer Precision GmbH + Co. KG, Essen, Germany) that circulated air at a rate of 600 cm^3 min^{-1} through a Nafion membrane tube (ME-110-03-12, Perma Pure Inc., Lakewood, NJ, U.S.A.) enclosed within a box of silica gel. CO_2 measurements consisted of a 30 s cycle during which air was pumped for 18 s and measurements were taken for 12 s with mean CO_2 concentrations logged. After 4-8 minutes, the flux chamber was lifted to reset inside-air CO_2 concentrations to ambient levels. This procedure was repeated 3 times for each sampling site yielding three linear regression slopes that describe the rise in CO_2 concentration over time. The mean(±standard deviation) coefficient of determination (R^2) of 846 individual measurements of the linear regression was 93±11%. Average coefficient of determination among triplicate slope measurements was 11±9%. The gas transfer velocity (*k*) was calculated using Fick's law of diffusion

$$k = \frac{F}{a\,(c_{wat} - c_{eq})} \quad \text{(A.1)}$$

where F is the CO_2 flux as estimated by the linear regression slopes, C_{wat} is the CO_2 concentration in water, C_{eq} is the CO_2 concentration of water if it was in equilibrium with ambient air calculated from measured air concentration and water temperature using Henry's constant and *a* is the chemical enhancement factor set to 1, as enhancement is negligible if pH < 8 (Wanninkhof and Knox, 1996). Molar CO_2 concentrations were derived from Bunsen solubility coefficients using water temperature-parameterizations in Weiss (1974). In-situ water temperature specific *k* values were normalized to 20˚C to yield k_{600} following Jähne et al. (1987) using Schmidt number parameterizations for water temperature according to Wanninkhof (1992). Reported errors in k_{600} were the standard errors of regression slopes of CO_2 concentration increases over time propagated for triplicate measurements at three sites per sub-reach (Fig. S3).

Propane injection experiments followed principles described in Wallin et al. (2011), with the following modifications. At a distance of 10-20 m upstream the uppermost sub-reach, liquefied petroleum gas (PC10, AGA gas AB, Luleå, Sweden) was injected into the stream at constant rates (2-8 l min^{-1}) and pressures (0.5-1 bar) using 2-3 aquarium gas diffusion stones (length=10 cm, diameter=5 cm). Flow rates were set by a propane regulator (Unicontrol 500, AGA gas AB, Luleå, Sweden) and monitored using a gas flow meter (ZYIA LZM, Yuyao Kingtai Instrument Co., Ltd., Zhejiang, China). Parallel to propane diffusion, we continuously injected a saturated sodium chloride (NaCl) solution using a peristaltic pump (FMI Lab Pump QBG, Fluid metering Inc., Syosset, NY, USA) and measured electrical conductivity every 10 s using conductivity loggers (HOBO U24, Onset Computer Corporation, Bourne, MA, U.S.A.) at five sites downstream, marking the upper and lower end of each of the sub-reaches (Fig. S1). Once conductivity reached a stable plateau (after 0.3-8 h), indicating propane saturation across

the whole stream reach, we took triplicate samples (50 ml) of bubble-free stream water at each site starting at the uppermost site using plastic syringes closed gas tight with three-way stopcocks. During extreme summer low flow, we varied propane injection sites in Lillsjölidtjärnen and Struptjärn to cover specific sub-reaches only, because travel times were too long for meaningful whole-reach injections. Within 4 hours after propane sampling, we replaced 20 ml of water by 20 ml of N_2 gas, shook syringes vigorously for 1 min and transferred the headspace gas to glass vials (22 ml; PerkinElmer Inc., Waltham, MA, U.S.A.) capped with butyl rubber stoppers (27232, Supelco Analytical, Bellefonte, PA, U.S.A.) by simultaneously withdrawing 20 ml of inside air. Within 24 hours after transfer to vials, the vial gas was analyzed on propane concentration by a gas chromatographer (Clarus 500, Perkin Elmer Inc., Waltham, MA, U.S.A.) equipped with a flame ionization detector. Propane concentrations in triplicate samples varied by 5±4% (mean±sd).

To account for dilution of propane by lateral water inputs, we estimated stream discharge for each sub-reach as $Q = \frac{s}{cal(c_s - c_b)}$, where s is the NaCl injection rate, c_s is the electrical conductivity when it has reached a stable plateau, c_b is the background electrical conductivity before salt injection and cal is a coefficient derived from in-situ calibrations linking electrical conductivity to NaCl mass. Stream discharge was constant along the reach in Övre Björntjärn but increased by a factor of 2.5 and 3 in Struptjärn and Lillsjölidtjärnen, respectively, from the upper- to the lowermost sub-reaches. The gas transfer coefficient (d^{-1}), the proportion of gas evaded over a specific reach per unit time, was calculated for propane using the log-ratio of discharge-corrected propane concentrations at the up- and downstream end of each sub-reach and converted to normalized gas transfer coefficients k_{600} following equations given in Wallin et al. (2011). Gas transfer coefficients were multiplied by the average sub-reach depth to obtain gas transfer velocities (m d^{-1}). Average sub-reach depth was obtained from six stream depth measurements taken at each of the three sites per sub-reach, where one measurement was taken at each of the six flux chamber edges (Fig. S1). Reported errors in k_{600} were propagated from standard errors of triplicate propane measurements and standard errors of the 18 stream depth measurements per sub-reach.

Text S5 Testing assumptions of the BACI analysis

To assess potential biases in the paired-BACI analysis of atmospheric gas fluxes due to pretreatment trends and autocorrelation, we tested the following assumptions (Stewart-Oaten et al. 1986): (1) Constancy of inter-lake differences in the before period, tested by linear mixed-effects models with "inter-lake difference" as the dependent variable, "sampling occasion" (Day of year) as a fixed effect and "pair" as a random effect on both slopes and intercepts; (2) Absence of significant positive first-order autocorrelation, tested by a Durbin-Watson test with the residuals of the model in (1) as the dependent variable and "sampling occasion" (Day of year) as the independent variable using the "dwtest" function of the R package "lmtest" (Zeileis and Hothorn, 2002); (3) Additivity of inter-lake differences in the before period, tested by linear mixed-effects models with "inter-lake differences" as the dependent variable, "inter-lake sums" as a fixed effect and "DOC-level" as a random effect on both slopes and intercepts.

Text S6 Error propagation

We accounted for uncertainties in BACI statistics for gas fluxes and gap-filled logger data by combining standard methods of error propagation and bootstrapping (Fig. S3). BACI analyses were run 10 times, with each observation sampled from a normal distribution defined by its mean estimate and propagated standard error. Standard errors were estimated as follows:

(1) For diffusive gas fluxes in streams, standard errors were propagated from errors due to gap filling of gas concentrations (standard error of 10 imputations, Text S3), the root-mean-square-error (rmse) of discharge rating curves and variability in k_{600} within sub-reaches and across triplicate flux chamber and propane injection experiments (Fig. S3A). Specifically, in corrections of flux chamber-derived k_{600} based on linear relationships

with propane-derived k_{600}, observations were weighted by the root mean square of the standard error of triplicate flux chamber and propane injection experiments. In predictions of k_{600} based on discharge, observations were weighted by the root mean square of the standard error of k_{600} and the rmse of discharge rating curves, where each error term was normalized to the respective mean estimate.

(2) For diffusive gas fluxes in lakes, standard errors were propagated from errors due to gap filling of gas concentrations (standard error of 10 imputations, Text S3) and from errors in modelled k_{600} (Fig. S3B). Errors in modelled k_{600} were derived from a separate bootstrap algorithm run 10 times, where all input variables were sampled from a normal distribution defined by the mean estimate and standard error derived from gap filling (as described in Text S3).

(3) For total CH_4 fluxes in lakes, errors were estimated from the area-weighted standard errors of depth-zone specific error estimates which in turn were the standard errors of fluxes of all chambers located therein (Fig. S3C).

(4) For weather variables and lake thermal characteristics standard errors were propagated from prediction errors of linear regressions used for gap filling (Fig. S3D).

References

Cole, J. J. and Caraco, N. F.: Atmospheric exchange of carbon dioxide in a low-wind oligotrophic lake measured by the addition of SF6, Limnol. Oceanogr., 43(4), 647–656, doi:10.4319/lo.1998.43.4.0647, 1998.

Heiskanen, J. J., Mammarella, I., Haapanala, S., Pumpanen, J., Vesala, T., Macintyre, S. and Ojala, A.: Effects of cooling and internal wave motions on gas transfer coefficients in a boreal lake, Tellus, Ser. B Chem. Phys. Meteorol., 66(1), 1–16, doi:10.3402/tellusb.v66.22827, 2014.

Honaker, J., King, G. and Blackwell, M.: Amelia II: a program for missing data, J. Stat. Softw., 45, 1–47, 2011.

Iribarne, J. V. and Godson, W. L.: Atmospheric Thermodynamics, 2nd ed., Springer., 1981.

Jähne, B. J., Münnich, K. O., Bösinger, R., Dutzi, A., Huber, W. and Libner, P.: On the Parameters Influencing Air-Water Gas Exchange, J. Geophys. Res., 92(C2), 1937–1949, doi:10.1029/JC092iC02p01937, 1987.

Johnson, M. S., Billet, M. F., Dinsmore, K. J., Wallin, M., Dyson, K. E. and Jassal, R. S.: Direct and continuous measurement of dissolved carbon dioxide in freshwater aquatic systems - method and applications, Ecohydrology, 3, 68–78, doi:10.1002/eco, 2010.

Klaus, M., Jonsson, A., Deininger, A., Geibrink, E. and Karlsson, J.: Weak response of greenhouse gas emissions to whole lake N enrichment, Limnol. Oceanogr., 63(S1), S340–S353, doi:10.1002/lno.10743, 2017.

Laudon, H., Taberman, I., Ågren, A., Futter, M., Ottosson-Löfvenius, M. and Bishop, K.: The Krycklan Catchment Study - A flagship infrastructure for hydrology, biogeochemistry, and climate research in the boreal landscape, Water Resour. Res., 49(10), 7154–7158, doi:10.1002/wrcr.20520, 2013.

Moore, R. D. D.: Introduction to Salt Dilution Gauging for Streamflow Measurement Part III: Slug injection using salt in solution, Streamline Watershed Manag. Bull., 8(2), 1–28, 2005.

Stewart-Oaten, A., Murdoch, W. W. and Parker, K. R.: Environmental impact assessment: "Pseudoreplication" in time?, Ecology, 67(4), 929–940, 1986.

Vachon, D. and Prairie, Y. T.: The ecosystem size and shape dependence of gas transfer velocity versus wind speed relationships in lakes, Can. J. Fish. Aquat. Sci., 70, 1757–1764, doi:10.1139/cfjas-2013-0241, 2013.

Wallin, M. B., Öquist, M. G., Buffam, I., Billett, M. F., Nisell, J. and Bishop, K. H.: Spatiotemporal variability of the gas transfer coefficient (K CO2) in boreal streams: Implications for large scale estimates of CO2 evasion, Global Biogeochem. Cycles, 25(3), 1–14, doi:10.1029/2010GB003975, 2011.

Wanninkhof, R.: Relationship Between Wind Speed and Gas Exchange Over the Ocean, J. Geophys. Res., 97(C5), 7373–7382, doi:10.1029/92JC00188, 1992.

Wanninkhof, R. and Knox, M.: Chemical enhancement of CO2 exchange in natural waters, Limnol. Oceanogr., 41(4), 689–697, doi:10.4319/lo.1996.41.4.0689, 1996.

Zeileis, A. and Hothorn, T.: Diagnostic Checking in Regression Relationships, R News, 2(3), 7–10 [online] Available from: http://cran.r-project.org/doc/Rnews/, 2002.

Figures

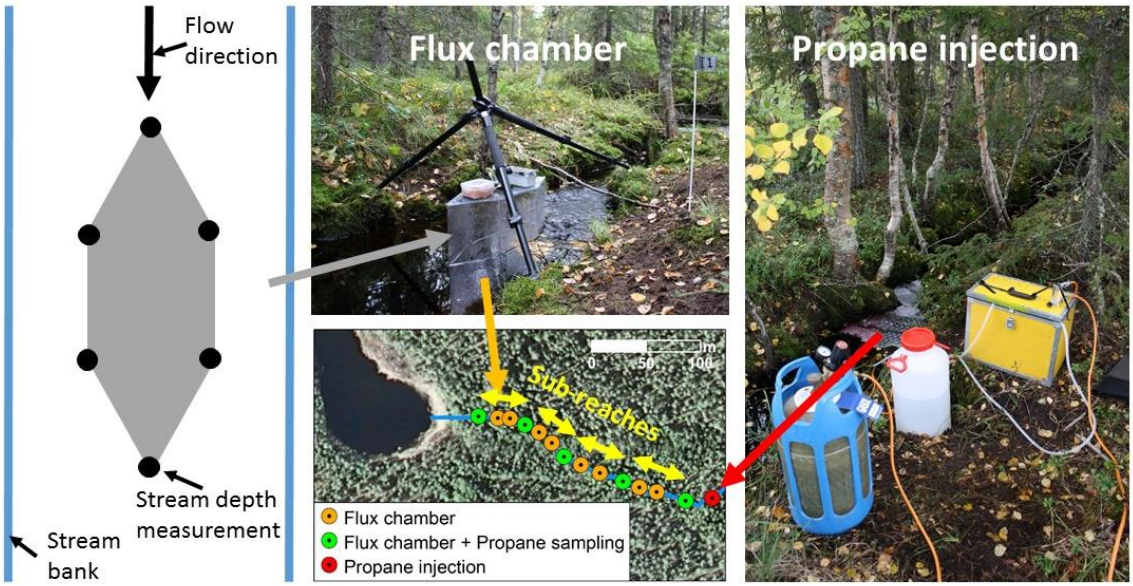

Figure S1: Field setup of gas transfer velocity measurements in streams by static flux chambers and propane injection experiments. The stream reach is divided into four sub-reaches above and below which propane concentrations were measured. Within each sub-reach, flux chamber measurements were done at three sites. At each site, stream depth was measured at the six edges of the flux chamber centered in the stream and aligned along flow direction.

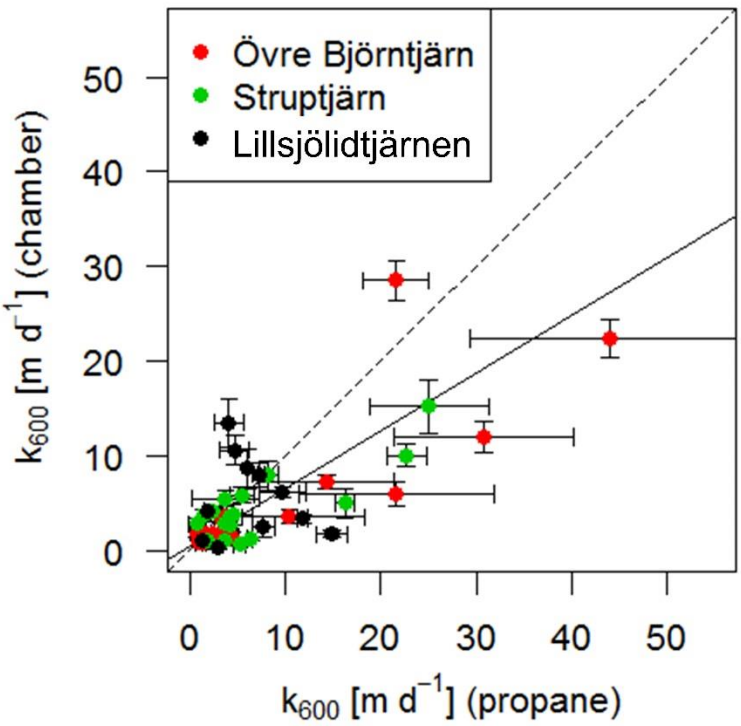

Figure S2: Sub-reach specific k_{600} derived from propane injection experiments (x) compared to the mean k_{600} of flux chamber measurements performed at three sites per sub-reach (y), given for three streams. The solid line shows the regression line of a linear mixed-effects model with "sub-reach" nested in "stream" as random effects on both slopes and intercepts where observations were weighted by the root mean square of measurement errors (se also Fig. S3A) expressed by error bars ($y=0.61x\pm0.13+0.53\pm0.43$, p-value of slope <0.001, $R^2=0.58$, n=46). The dotted line shows a hypothetical 1:1 relationship.

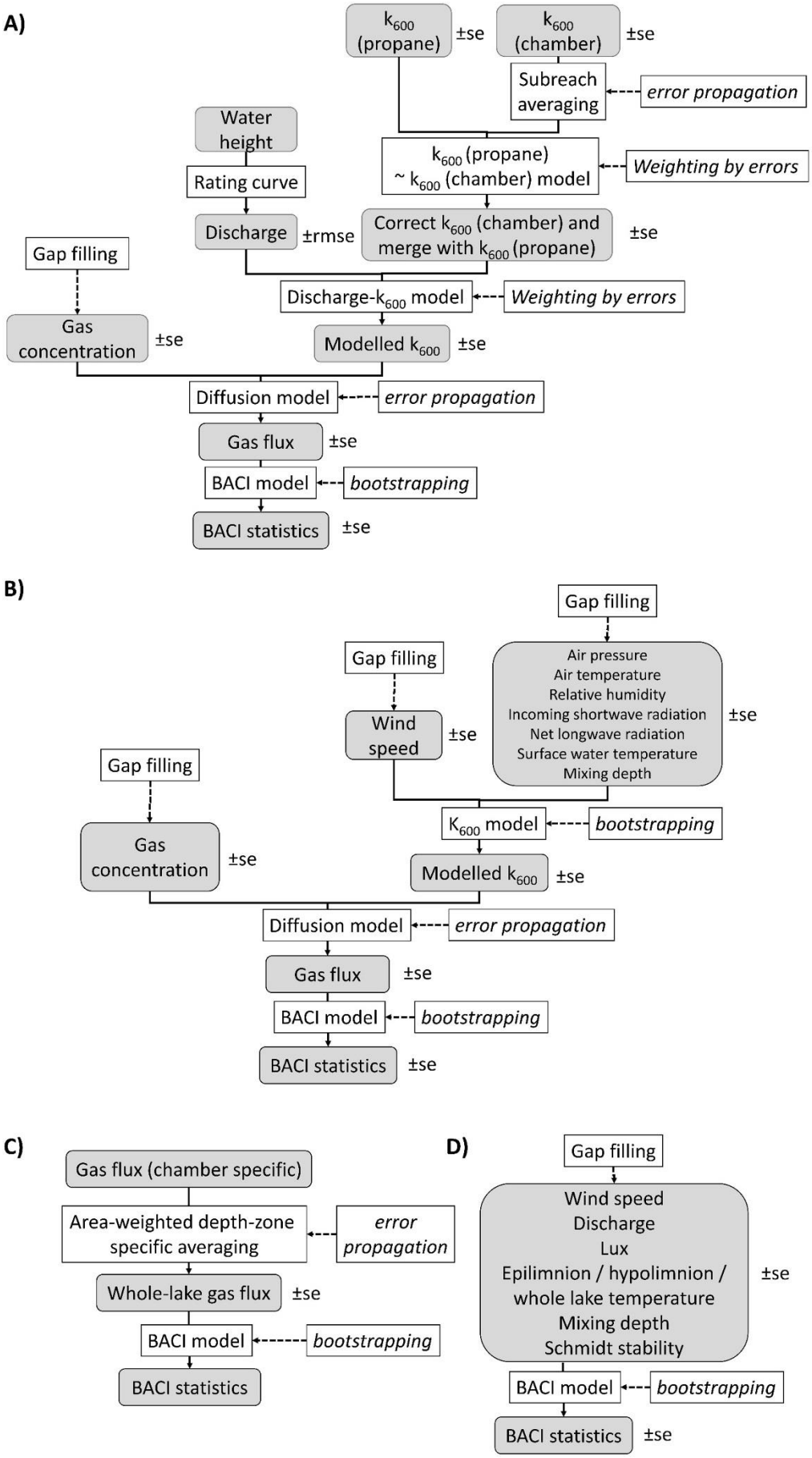

Figure S3: Overview of the errors associated with estimates of diffusive gas fluxes across the air-water interface in A) streams and B) lakes, C) total lake CH_4 flux and D) other continuously measured physical parameters. Errors were propagated following standard rules and bootstrapping (Text S6). For gap-filling procedures, see Table S2. Abbreviations: "BACI"=Before/After-Control/Impact, "k_{600}" = gas-transfer velocity for CO_2 at 20˚C. "se"=standard error, "rmse" = root mean square error.

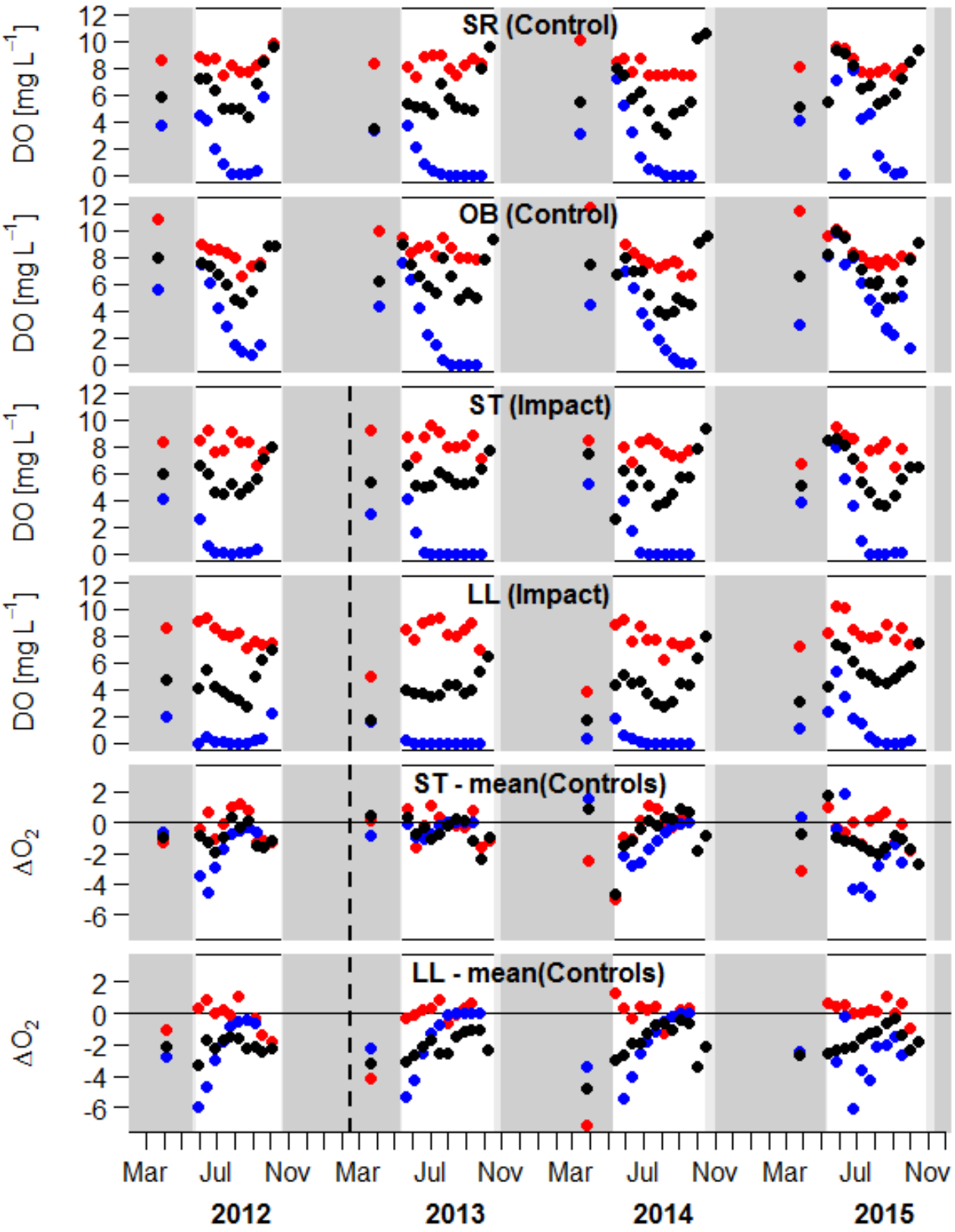

Figure S4: Time series of depth-integrated O_2 concentrations based on biweekly profile measurements (red=epilimnion, blue=hypolimnion, black=whole lake). Given are absolute values and differences (ΔO_2) between impact and control lakes. Bars show the minimum (dark grey) and maximum (light grey) lake ice extent. The vertical dashed line marks the timing of forest clear-cutting. Units are consistent across all panels. Abbreviations: SR=Stortjärn, OB=Övre Björntjärn, ST=Struptjärn, LL=Lillsjölidtjärnen.

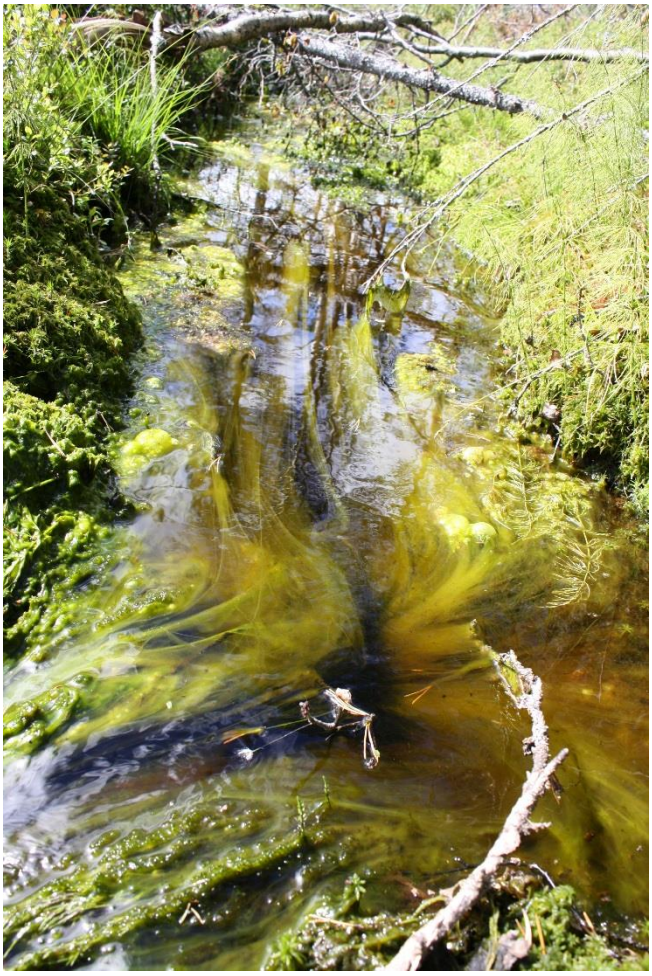

Figure S5: Algae bloom observed in July 2013 in the inlet stream of Struptjärn after forest clear-cutting.

Tables

Table S1: Air temperatures and precipitation sums during the study period (June-September 2012-2015), given as means±sd across the study catchments.

Variable	Unit	2012	2013	2014	2015
Air temperature	˚C	11.1±0.3	12.7±0.3	12.8±0.3	11.6±0.3
Precipitation	mm	342±12	321±26	245±42	274±29

Table S2: Details on the extent and filling of gaps in continuously logged data. Given are the length of gaps as a proportion of the total data set, the mean±sd gap length, the gap filling method, the training data used for gap filling and the mean R^2 value of the linear regressions used for gap filling. Training data included all data collected in the year the gap occurred.

			gap length [d]				
Parameter	System	Proportion of gaps	mean	sd	Gap filling method	Training data	R^2
CO_2	Lake	0.07	8	7	Multivariate imputation[#]	Co-variates*	-
CO_2	Stream	0.03	6	8	Linear interpolation	Spot measurements	-
Wind speed	Open mire	0.12	39	10	Multivariate imputation[#]	All other weather stations	-
Air temperature	Open mire	0.11	41	47	Linear regression	Nearest weather station	0.96
Air pressure[†]	Open mire	0.10	32	46	Linear regression	Nearest weather station	0.99
Relative humidity[‡]	Open mire	0.09	85	50	Linear regression	Nearest weather station	0.83
Lux	Lake	0.04	25	27	Linear regression	Nearest lux logger	0.83
Lux	Stream	0.11	23	8	Linear regression	Nearest lux logger	0.63
Surface Temperature	Lake	0.04	27	20	Linear regression	Replicate lake	0.93
Epilimnion temperature	Lake	0.04	27	20	Linear regression	Replicate lake	0.96
Hypolimnion temperature	Lake	0.04	27	20	Linear regression	Replicate lake	0.89
Whole lake temperature	Lake	0.04	27	20	Linear regression	Replicate lake	0.93
Schmidt Stability	Lake	0.04	27	20	Linear regression	Replicate lake	0.94
Mixing depth	Lake	0.04	27	20	Linear regression	Replicate lake	0.60

[†]not measured in Stortjärn; modelled using bathymetric formula

[‡]not measured in Struptjärn; mean and error estimates assumed to be the same as in Övre Björntjärn

[#]Honaker et al. 2011

*see Klaus et al. (2017)

Table S3: Parameter estimates of sub-reach-specific linear regression models that predict k_{600} (m d^{-1}) based on discharge (L s^{-1}). Each observation was weighted by the root mean square of their standard errors. Abbreviations: se=standard error, t=t-value, p=p-value, NA=Not available, n=number of observations. Statistically significant p-values (<0.05) are highlighted bold.

				Intercept				Slope					
Catchment	Sub-reach	Distance to lake [m]	n	mean	se	t	p	mean	se	t	p	R^2	rse
Övre Björntjärn	1	87	19	1.470	1.297	1.13	0.27	0.339	0.062	5.46	**0.00**	0.64	4.24
Övre Björntjärn*	2	201	18	0.000	NA	NA	NA	0.262	0.027	9.65	**0.00**	0.85	1.77
Övre Björntjärn	3	225	17	0.956	0.514	1.86	0.08	0.136	0.028	4.84	**0.00**	0.61	1.68
Övre Björntjärn†	4	259	17	0.956	0.514	1.86	0.08	0.136	0.028	4.84	**0.00**	0.61	1.68
Övre Björntjärn‡	5	300	2	1.635	0.548	NA	NA	NA	NA	NA	NA	NA	NA
Struptjärn*	1	63	13	0.000	NA	NA	NA	0.343	0.056	6.10	**0.00**	0.76	2.38
Struptjärn	2	103	15	1.591	0.288	5.53	0.00	0.187	0.034	5.44	**0.00**	0.69	1.13
Struptjärn	3	140	13	0.432	0.698	0.62	0.55	0.796	0.061	12.97	**0.00**	0.94	1.63
Struptjärn	4	197	13	0.720	0.754	0.95	0.36	0.332	0.088	3.78	**0.00**	0.56	2.17
Struptjärn**	5	283	13	0.720	0.754	0.95	0.36	0.332	0.088	3.78	**0.00**	0.56	2.17
Lillsjölidtjärnen	1	46	10	1.536	1.284	1.20	0.27	0.591	0.237	2.50	**0.04**	0.44	2.28
Lillsjölidtjärnen	2	90	10	1.475	0.691	2.13	0.07	1.120	0.185	6.07	**0.00**	0.82	1.85
Lillsjölidtjärnen*	3	134	9	0.000	NA	NA	NA	1.966	0.171	11.50	**0.00**	0.94	2.84
Lillsjölidtjärnen	4	195	10	0.578	0.300	1.93	0.09	1.405	0.135	10.37	**0.00**	0.93	1.80
Lillsjölidtjärnen†	5	256	10	0.578	0.300	1.93	0.09	1.405	0.135	10.37	**0.00**	0.93	1.80

* intercept constrained to zero

†model of n-th subreach assumed to be the same as model of (n-1)th subreach, motivated by their similar morphology

‡k_{600} assumed to be constant (mean of 6 flux chamber measurements), because discharge variations were negligible and greatly buffered at this mire site

Table S4: Physicochemical characteristics of lake-, stream-, and groundwater at control and impact sites before and after site preparation (year 2012 and 2015, respectively). Given are also the estimated effect size (linear mixed effects model slope), its standard errors (se), degrees of freedom (df), t- and p-values and Cohen'D, summarized as arithmetic means over ten bootstrap runs that account for uncertainty from gap filling. This uncertainty is expressed as bootstrap standard errors (bse) of p-values. Statistically significant p-values (<0.05) are highlighted bold. Water levels [cm] are relative to the soil surface. Groundwater data refers to depth-integrated locations (5-105 cm). Abbreviations: Epi=Epilimnion, Hypo=hypolimnion, z_{mix}= mixing depth [m], DOC=Dissolved organic carbon concentration [mg L^{-1}], TN=total nitrogen concentration [µg L^{-1}], DIN=dissolved inorganic nitrogen concentration [µg L^{-1}], a_{420}=spectral absorbance at 420 nm [m^{-1}].

			Before					After					Effect size (Slope)						
			Control		Impact			Control		Impact									
Variable	System	Unit	mean	se	mean	se	n	mean	se	mean	se	n	mean	se	df	t	p	bse	Cohen's D
Wind speed	Open mire*	m s^{-1}	1.8	0.1	1.0	0.1	244	2.0	0.1	0.9	0.0	244	-0.1	0.1	485	-1.3	0.24	0.04	-0.16
Discharge	Stream*	L s^{-1}	40.9	3.4	4.2	0.4	244	32.9	2.6	4.7	0.4	244	0.2	0.3	485	0.5	0.64	0.02	0.08
Water level	Groundwater	cm	34.5	1.8	34.6	1.8	17	42.4	3.0	39.1	2.9	18	-57.4	51.6	32	-1.1	0.27	-	-0.49
Lux	Lake	lux	31199	1096	22426	897	244	33677	1013	22393	888	244	-2518	2166	485	-1.2	0.25	0.00	-0.11
	Stream*		5952	251	3398	168	244	6199	192	10572	614	244	0.2	0.2	485	1.2	0.25	0.01	0.96
Temperature	Stream	˚C	8.6	0.1	8.1	0.1	244	8.2	0.1	7.9	0.1	244	0.2	0.2	485	1.3	0.19	0.00	0.07
	Lake Epi		14.4	0.2	14.8	0.2	245	14.8	0.2	15.2	0.2	244	0.0	0.2	486	-0.2	0.81	0.00	-0.03
	Lake Hypo		7.0	0.0	6.0	0.1	227	9.3	0.0	7.1	0.1	238	-1.3	0.4	462	-3.5	**0.00**	0.00	-0.68
	Whole Lake‡		11.1	0.1	10.7	0.1	245	12.2	0.1	11.4	0.1	244	-0.4	0.0	486	-9.8	**0.00**	0.00	-0.24
Z_{mix}	Lake*	m	1.8	0.1	1.7	0.1	227	2.0	0.1	1.6	0.1	238	-0.4	0.1	462	-4.1	**0.00**	0.00	-0.26
Schmidt Stability	Lake		13.3	0.6	12.8	0.5	245	11.2	0.5	12.6	0.4	244	1.8	0.6	486	3.0	**0.00**	0.00	0.25
Oxygen	Lake Epi	mg L^{-1}	8.2	0.1	8.1	0.2	20	8.3	0.2	8.2	0.2	20	-0.1	0.4	37	-0.2	0.82	-	-0.05
	Lake Hypo‡		2.2	0.5	0.8	0.4	17	4.3	0.5	1.7	0.5	18	-0.7	1.1	32	-0.7	0.52	-	-0.18
	Whole Lake		6.4	0.3	5.1	0.3	20	7.2	0.4	5.7	0.3	20	-0.2	0.5	37	-0.3	0.77	-	-0.08
DOC	Lake Epi	mg L^{-1}	22	1.0	18	0.9	20	22	0.9	19	1.2	20	1.2	2.9	37	0.4	0.67	-	0.18
	Stream		29	0.9	28	1.4	59	25	1.1	24	1.6	75	1.3	1.8	131	0.7	0.47	-	0.07
	Groundwater		67	3.0	77	2.4	14	55	5.7	66	6.7	10	1.9	8.5	21	0.2	0.82	-	0.06
TN	Lake Epi	µg L^{-1}	409	15.7	367	14.3	20	427	13.7	401	19.6	20	16.2	48.3	37	0.3	0.74	-	0.15
	Stream†		498	13.5	595	35.3	58	450	17.0	486	23.6	75	-49.6	52.1	130	-1.0	0.34	-	-0.10
	Groundwater		1572	180.4	1798	83.8	14	1288	167.2	1575	150.9	10	58.3	256.5	21	0.2	0.82	-	0.05
DIN	Lake Epi	µg L^{-1}	20	1.6	19	2.0	20	15	1.3	10	1.4	20	-4.7	3.3	37	-1.4	0.17	-	-0.26

	Stream		21	2.0	23	2.2	57	16	0.8	30	1.9	73	10.3	4.4	127	2.4	**0.02**	-	0.25
	Groundwater†		467	98.9	523	42.4	13	411	95.3	501	67.5	7	4.7	166.3	17	0.0	0.98	-	0.01
pH	Lake Epi†*		4.2	0.1	5.1	0.1	20	4.9	0.0	5.4	0.0	20	0.00	0.00	37	1.0	0.31	-	0.25
	Stream*		3.9	0.1	4.4	0.1	20	4.6	0.0	4.6	0.0	20	0.00	0.00	37	3.1	**0.00**	-	0.36
a_{420}	Lake Epi	m^{-1}	12.4	0.4	9.3	0.6	20	12.4	0.3	10.0	0.7	20	0.01	0.02	37	0.4	0.70	-	0.14
	Stream		15.1	0.4	13.6	0.7	53	12.5	0.3	12.1	0.7	76	0.02	0.01	126	1.7	0.08	-	0.16

*LME estimates based on log-transformed data

‡Assumption on constancy of paired differences in before-period not met

†Assumption on non-additivity of paired differences in before-period not met

#mean and LME estimates based on H+ concentrations, se based on pH value

Table S5: Seasonal mean(±se) concentrations [µM] of DIC and CH_4 in groundwater in control and impact catchments before and after site preparation in impact catchments (years 2012 vs. 2015). Given are also linear mixed effects model slope estimates of the effects of site preparation (mean), their standard errors (se), degrees of freedom (df), t- and p-values and Cohen'D. Statistically significant p-values (<0.05) are highlighted bold.

		Before					After										
		Control		Impact			Control		Impact			Effect size (Slope)					
Substance	Soil depth [cm]	mean	se	mean	se	n	mean	se	mean	se	n	mean	se	df	t	p	Cohen's D
DIC	37.5 - 42.5	992	90	957	99	17	1446	138	1949	153	17	518	249	31	2.1	**0.046**	0.61
DIC	5 - 105	1380	172	1624	221	18	2062	196	3072	285	19	799	971	34	0.8	0.42	0.52
CH_4	37.5 - 42.5	23.7	7.0	11.4	4.2	17	6.8	1.8	69.1	21.5	16	68.5	69.1	30	1.0	0.33	1.19
CH_4	5 - 105	82.0	23.4	88.0	22.8	18	207.6	41.1	406.8	62.1	19	207.9	279.2	34	0.7	0.46	1.07

Table S6: Seasonal mean(±se) concentrations of dissolved CO_2, CH_4 and N_2O in stream and lake water in control and impact catchments before and after clear-cutting (years 2012 vs. 2013-2015) and site preparation (years 2012 vs. 2015). Given is also the estimated effect size (linear mixed-effects model slope), its standard error (se), degrees of freedom (df), t- and p-values and Cohen'D. Statistically significant p-values (<0.05) are highlighted bold. Note that parameter estimates are based on log+n transformed data, where n is the smallest number that leads to positive normal values. Abbreviations: Logger=Daily mean of 2-hourly measurement, Spot=Biweekly spot measurement.

					Before					After					Effect size (Slope)					
					Control		Impact			Control		Impact								
Gas	Unit	Method	System	Treatment	mean	se	mean	se	n	mean	se	mean	se	n	mean	se	df	t	p	Cohen's D
CO_2†	µM	Logger	Lake	Clear-cut	103.0	2.2	109.2	3.2	242	95.0	1.5	104.3	1.8	726	0.27	0.15	965	1.74	0.08	0.05
				Site preparation	103.0	2.2	109.2	3.2	242	96.8	1.8	97.0	2.2	242	0.02	0.33	481	0.07	0.95	-0.10
CO_2	µM	Logger	Stream	Clear-cut	269.2	6.9	314.4	6.6	246	346.6	4.9	349.4	3.1	739	-0.13	0.02	982	-5.85	**0.00**	-0.28
				Site preparation	269.2	6.9	314.4	6.6	246	313.9	6.7	328.8	4.8	247	-0.10	0.03	490	-3.70	**0.00**	-0.20
CH_4†	µM	Spot	Lake	Clear-cut	0.3	0.0	0.8	0.2	19	0.4	0.1	1.1	0.2	56	0.09	0.30	72	0.30	0.76	0.17
				Site preparation	0.3	0.0	0.8	0.2	19	0.3	0.1	0.8	0.2	20	0.02	0.41	36	0.05	0.96	-0.01
CH_4‡,#	µM	Spot	Stream	Clear-cut	0.8	0.1	0.2	0.0	18	3.4	1.0	3.1	2.6	58	-0.17	0.26	73	-0.65	0.52	0.01
				Site preparation	0.8	0.1	0.2	0.0	18	1.2	0.2	0.1	0.1	20	-0.18	0.12	35	-1.48	0.15	-0.01
N_2O	nM	Spot	Lake	Clear-cut	15.2	1.1	16.7	1.4	19	13.3	0.8	12.2	0.7	32	-0.15	0.12	48	-1.26	0.21	-0.04
N_2O	nM	Spot	Stream	Clear-cut	20.0	1.9	22.2	2.6	18	15.7	1.2	18.2	1.4	32	0.18	0.20	47	0.87	0.39	0.01

†Assumption on non-additivity of paired differences in before-period not met

‡Assumption on constancy of paired differences in before-period not met

#one outlier removed

Table S7: Seasonal mean(±se) fluxes [mmol m^{-2} d^{-1}] of dissolved CO_2 and CH_4 across the interface between lakes or streams and the atmosphere in control and impact catchments before and after site preparation (years 2012 vs. 2015). Given is the estimated effect size of site-preparation (linear mixed-effects model slope), its standard error (se), degrees of freedom (df), t- and p-values and Cohen'D, summarized as arithmetic means over ten bootstrap runs that account for uncertainty from gap filling and gas flux models (see Fig. S3). This uncertainty is expressed as bootstrap standard errors (bse) of p-values. For lake-atmosphere fluxes, estimates based on three different *k* models are shown. Note that parameter estimates are based on log+n transformed data, where n is the smallest number that leads to positive normal values. Abbreviations: Logger=Daily mean of 2-hourly measurement, Spot=Biweekly spot measurement. Cole=Cole and Caraco (1998), Vachon=Vachon and Prairie (2013), Heiskanen=Heiskanen et al. (2014).

				Before					After					Effect size (Slope)						
				Control		Impact			Control		Impact									
Gas	System	Method	k model	mean	se	mean	se	n	mean	se	mean	se	n	mean	se	df	t	p	bse	Cohen's D
CO_2	Lake	Logger	Cole	52.8	2.0	43.0	1.4	242	50.4	1.4	37.2	0.9	242	-0.11	0.30	481	-0.4	0.73	0.02	-0.08
CO_2	Lake	Logger	Vachon	75.6	2.3	58.8	1.9	242	71.7	1.8	51.1	1.3	242	-0.09	0.31	481	-0.3	0.78	0.02	-0.07
CO_2†	Lake	Logger	Heiskanen	98.1	4.0	76.2	3.3	242	98.5	3.5	69.2	2.5	242	-0.06	0.23	481	-0.3	0.79	0.04	-0.08
CO_2	Stream	Logger	This study	352.8	30.5	86.8	4.6	246	313.8	32.6	93.5	5.7	247	0.10	0.23	490	0.5	0.66	0.07	0.07
CH_4†	Lake	Spot	Cole	0.18	0.02	0.33	0.07	19	0.24	0.13	0.33	0.14	20	-0.09	0.30	36	-0.3	0.76	0.02	-0.10
CH_4†	Lake	Spot	Vachon	0.24	0.02	0.48	0.11	19	0.31	0.17	0.45	0.21	20	-0.13	0.32	36	-0.4	0.68	0.02	-0.09
CH_4	Lake	Spot	Heiskanen	0.28	0.04	0.39	0.10	19	0.45	0.26	0.40	0.27	20	-0.15	0.29	36	-0.5	0.62	0.05	-0.17
CH_4†	Stream	Spot	This study	1.26	0.38	0.07	0.07	19	0.76	0.19	-0.05	0.03	20	0.08	0.14	36	0.6	0.56	0.08	0.12

†Assumption on non-additivity of paired differences in before-period not met

Table S8: Linear mixed effects model estimates of the effects of forest clear-cutting on CO_2 and CH_4 fluxes across the stream-atmosphere interface as shown in Figure 8. Given are the estimated effect size (model slope), its standard error (se), degrees of freedom (df), t- and p-values and Cohen'D, as arithmetic means over ten bootstrap runs that account for uncertainty from gap filling and gas flux models (see Fig. S3). Uncertainty is expressed as bootstrap standard errors (bse) of p-values. Parameter estimates are based on log+n transformed data, where n is the smallest number that leads to positive normal values.

				Effect size (Slope)						
Figure	Gas	Catchment	Distance to lake [m]	mean	se	df	t	p	bse	Cohen's D
8B)	CO_2	Lillsjölidtjärnen	46	0.21	0.56	28.00	0.39	0.70	0.07	0.20
8B)	CO_2†	Lillsjölidtjärnen	90	0.34	0.44	28.00	0.79	0.45	0.05	0.19
8B)	CO_2	Lillsjölidtjärnen	134	-0.01	0.44	28.00	-0.01	0.78	0.05	0.07
8B)	CO_2	Lillsjölidtjärnen	195	0.11	0.37	28.00	0.29	0.77	0.05	0.15
8B)	CO_2	Lillsjölidtjärnen	256	-0.37	0.38	28.00	-0.98	0.38	0.07	-0.36
8B)	CO_2†	Struptjärn	63	0.47	0.50	27.00	0.96	0.36	0.04	0.23
8B)	CO_2	Struptjärn	103	0.33	0.51	27.00	0.63	0.56	0.07	0.21
8B)	CO_2	Struptjärn	140	0.13	0.49	27.00	0.31	0.72	0.07	0.14
8B)	CO_2	Struptjärn	197	0.23	0.41	27.00	0.58	0.58	0.06	0.21
8B)	CO_2	Struptjärn	283	-0.10	0.38	27.00	-0.21	0.71	0.04	-0.05
8D)	CH_4†	Lillsjölidtjärnen	46	-0.04	0.32	26.00	-0.14	0.88	0.02	-0.66
8D)	CH_4†	Lillsjölidtjärnen	90	0.07	0.23	25.00	0.23	0.81	0.04	0.07
8D)	CH_4	Lillsjölidtjärnen	134	-0.15	0.32	25.00	-0.47	0.64	0.03	-0.57
8D)	CH_4†	Lillsjölidtjärnen	195	-0.13	0.34	25.00	-0.40	0.70	0.02	-0.50
8D)	CH_4†	Lillsjölidtjärnen	256	-0.31	0.65	26.00	-0.48	0.64	0.02	-0.76
8D)	CH_4	Struptjärn	63	0.07	0.19	24.00	0.33	0.69	0.06	-0.35
8D)	CH_4	Struptjärn	103	-0.05	0.56	24.00	-0.09	0.69	0.05	-0.11
8D)	CH_4	Struptjärn	140	-0.07	0.27	24.00	-0.26	0.71	0.06	-0.72
8D)	CH_4†	Struptjärn	197	-0.03	0.26	24.00	-0.02	0.81	0.05	-0.35
8D)	CH_4†	Struptjärn	283	-0.39	0.68	24.00	-0.59	0.56	0.03	-0.83

†Assumption on non-additivity of paired differences in before-period not met